A Mixed-Effects Model to Predict COVID-19 Hospitalizations Using Wastewater Surveillance

Maria L. Daza–Torres[1, +], J. Cricelio Montesinos-López[1, +], Angel N. Desai[2], Colleen C. Naughton[3], Heather N. Bischel[4], and Miriam Nuño[1,*]

[1] *Department of Public Health Sciences, University of California Davis, California 95616, United States*

[2] *Department of Internal Medicine, University of California Davis, Sacramento, California 95817, United States*

[3] *Department of Civil and Environmental Engineering, University of California Merced, Merced, California 95343, United States*

[4] *Department of Civil and Environmental Engineering, University of California Davis, Davis, California 95616, United States*

[+] *co-first author*

[*] *corresponding author: mnuno@ucdavis.edu*

Abstract

During the COVID-19 pandemic, many countries and regions investigated the potential use of wastewater-based disease surveillance as an early warning system. Initially, methods were created to detect the presence of SARS-CoV-2 RNA in wastewater. Investigators have since conducted extensive studies to examine the link between viral concentration in wastewater and COVID-19 cases in areas served by sewage treatment plants over time. However, only a few reports have attempted to create predictive models for hospitalizations at county-level based on SARS-CoV-2 RNA concentrations in wastewater. This study implemented a linear mixed-effects model that observes the association between levels of virus in wastewater and county-level hospitalizations. The model was then utilized to predict short-term county-level hospitalization trends in 21 counties in California based on data from March 21, 2022, to May 21, 2023. The modeling framework proposed here permits repeated measurements as well as fixed and random effects. The model that assumed wastewater data as an input variable, instead of cases or test positivity rate, showed strong performance and successfully captured trends in hospitalizations. Additionally, the model allows for the prediction of SARS-CoV-2 hospitalizations two weeks ahead. Forecasts of COVID-19 hospitalizations could

provide crucial information for hospitals to better allocate resources and prepare for potential surges in patient numbers.

Keywords: SARS-CoV-2; COVID–19; Hospitalizations; Wastewater-based epidemiology; Wastewater-based disease surveillance; Linear mixed-effects model

1 Introduction

Wastewater-based disease surveillance (WDS) is a valuable tool for identifying and monitoring the spread of infectious diseases within a community. By detecting the presence of SARS-CoV-2 RNA in municipal sewer systems, WDS systems can provide early detection of outbreaks and track changes in the concentration of the virus over time: WDS can also be used to identify the spread of new variants when they emerge. Wastewater surveillance was used effectively prior to the COVID-19 (Coronavirus Disease 2019) pandemic, most notably as a tool to monitor and respond to poliovirus and to assess the presence of pharmaceutical and illicit drugs (Paul et al., 1940; Trask et al., 1938). The COVID-19 pandemic led to widespread implementation of WDS in communities across the United States. The approach has proven to be a cost-effective method for tracking COVID-19 and other infectious diseases (To et al., 2010; Hughes et al., 2022; Boehm et al., 2023a; Kumblathan et al., 2021). To bolster the nation's capacity to monitor SARS-CoV-2 effectively, the US Centers for Disease Control and Prevention (CDC) launched the National Wastewater Surveillance System (NWSS) in September 2020, establishing over 1250 sampling sites across the US that encompassed more than 133 million people by October 2022. An essential factor contributing to the success of WDS is the extensive coverage of municipal wastewater collection systems, which connects approximately eighty percent of households in the United States.

In contrast, conducting widespread testing in a community requires substantial testing capacity, including access to testing kits, trained personnel, and testing facilities. Implementing community-wide testing can be financially burdensome, especially in resource-constrained settings. Even with adequate testing capacity, achieving high participation in testing can be challenging. When individuals get tested for a disease, their test-seeking and preventive behaviors can lead to biases. This can make the tested population less representative and affect the accuracy of disease prevalence esti-

mates. Therefore, relying solely on confirmed cases to determine disease prevalence in a community can lead to biased estimates (Daza-Torres et al., 2023).

In order to reduce the biases introduced by testing practices, the test positivity rate (TPR) emerges as a crucial alternate measure. The TPR is the proportion of individuals who have tested positive for COVID-19 relative to the total number of tests administered. TPR has been used as a valuable alternative metric to track the spread of COVID-19 and assess the disease's prevalence compared to the number of tests being conducted (Dallal et al., 2021; Dowdy and D'Souza, 2020). TPR has been demonstrated to reliably correlate with hospitalizations and intensive care units (Fenga and Gaspari, 2021; Montesinos-López et al., 2021). However, the interpretation and use of the TPR can be challenging in certain contexts, as it relies on accurate and comprehensive testing data, which may be hindered by factors such as limited testing capacity, variable testing practices, and variations in reporting standards.

One solution to the challenges faced in estimating disease prevalence in a community is through the use of WDS. This approach is relatively simple and accurate in gathering data from both symptomatic and asymptomatic individuals across an entire community. WDS provides a more accurate estimation of disease prevalence as it represents a sample of the population regardless of individual testing behaviors or access to healthcare. Numerous studies have observed a strong correlation between SARS-CoV-2 RNA concentrations in wastewater with the number of daily new cases in corresponding wastewater treatment plants catchment areas and, more recently, with the TPR (Montesinos-López et al., 2023).

Galani et al. (2022) and Kadonsky et al. (2023) offer examples of correlations between wastewater data and hospitalizations, with a time lag typically ranging from 8 to 14 days. Galani et al. (2022) implemented an artificial neural network model that combines clinical test results (COVID-19-positive cases) and wastewater concentrations to model new hospital and ICU admissions. These findings emphasize the potential of wastewater surveillance to improve preparedness and response to the spread of infectious diseases.

Building upon this knowledge, we propose using a linear mixed-effects model (LMM) to predict COVID-19 hospitalizations at a county-level by examining viral concentrations found in wastewater. Our analysis covers 21 counties in California for which wastewater data for COVID-19 is

reported by WastewaterSCAN, a national WDS program that began in California in 2020 (Boehm et al., 2023b). The results of the present study thus offer an extensive assessment of correlations between wastewater data and hospitalization rates and demonstrate the broad applicability of the hospitalization forecasting models.

2 Materials and Methods

The analytical framework was developed using data from twenty-one counties across California, USA, which actively monitor wastewater. The analysis includes clinical and wastewater data from March 21, 2022, to May 21, 2023, covering three waves of the COVID-19 pandemic. We defined the first wave period from March 21, 2022, to October 15, 2022; the second wave starts on October 16, 2022, and ends on February 4, 2023; and the third wave starts on February 5, 2023, and ends until the end of the study period, May 21, 2023 (see Figure 1).

2.1 Data Sources

Clinical Data

We used publicly available data for daily COVID-19 cases and hospitalization at the county level from the Official California State Government website, which provided the COVID-19 data from the California Health & Human Services Agency (CHHS). Hospitalization counts represent the number of patients hospitalized in an inpatient bed with a laboratory-confirmed COVID-19 diagnosis. It is important to note that some hospitalization data may involve individuals admitted to the hospital for reasons unrelated to COVID-19 but who tested positive during their hospital stay. The count includes all inpatients, including those in ICU and Medical/Surgical units, but excludes patients waiting for an inpatient bed in affiliated clinics, outpatient departments, emergency departments, and overflow locations.

The number of positive COVID-19 cases is determined by the total count of molecular tests that were positive using polymerase chain reaction (PCR) assays. We considered both “Total Tests” and “Positive Tests”, which reflect the cumulative totals based on the collection date. There is typically

a delay between the date of specimen collection and when the test results are reported, which could impact real-time forecasts of hospitalizations as positive tests are reported.

Hospital admissions and COVID-19 cases were aggregated weekly. To calculate population-level hospitalization rates and cases for a county, we take the number of hospital admissions and new cases in the past 7 days, divide it by the population in that same county, and then multiply the result by 100,000. These metrics make it easier to compare data across different counties (refer to Figure 1). We will refer to the standardized hospitalization as "hospitalization rate" moving forward.

To calculate the TPR for a specific county, the number of positive COVID-19 tests from the past 7 days is divided by the total number of tests conducted in that county during that same time frame.

Wastewater Data

Wastewater data used in this study are available publicly through the Verily Wastewater Testing Dashboard (Verily). Counties with at least one wastewater treatment plant reporting wastewater data with data collection started before January 2023 were included in this study. San Benito County was excluded from the analysis due to the low quality of hospital data.

The pre-analytical and analytical methods used for measuring the SARS-CoV-2 RNA N gene and PMMoV are registered and previously described in peer-reviewed publications (Boehm et al., 2023b). WastewaterSCAN (WastewaterSCAN) provides testing, sampling supplies, and free shipping to participating treatment plants. Sewage treatment plants receive kits to sample primary sludge or wastewater influent three times or more weekly and shipping for lab analysis at no cost. Verily makes results available through its dashboard within 48 hours of receiving samples (Verily).

SARS-CoV-2 concentrations are reported for each location as viral RNA genome copies per gram of dry wastewater solids (gc/g dry solids). Pepper mild mottle virus (PMMoV), frequently used for normalizing SARS-CoV-2 concentrations in WDS, is also reported as process control as RNA copies per gram of dry wastewater solids. The SARS-CoV-2 viral load is normalized by the PMMoV concentration, resulting in the dimensionless metric N/PMMoV. The N gene is present in all variants of the virus. The analytical method applied is highly sensitive such that non-detects of

SARS-CoV-2 were rare over the time period and geographic region for which data was obtained. Non-detects are included as 0 gc/g dry solids. Figure 1 shows the N/PMMoV and hospitalization rate per 100K population.

To analyze the relationship between hospitalization rates and SARS-CoV-2 normalized wastewater concentrations, we used data from the wastewater treatment plant serving the highest population in each county. We calculated the weekly average N/PMMoV concentrations by dividing the sum of concentrations by the number of samples collected during that week.

The analyses of this study used publicly available data and do not contain any private health information. As a result, our study is exempt from ethical review and the requirement for informed consent, according to the Common Rule 45 CFR46.102 guidelines.

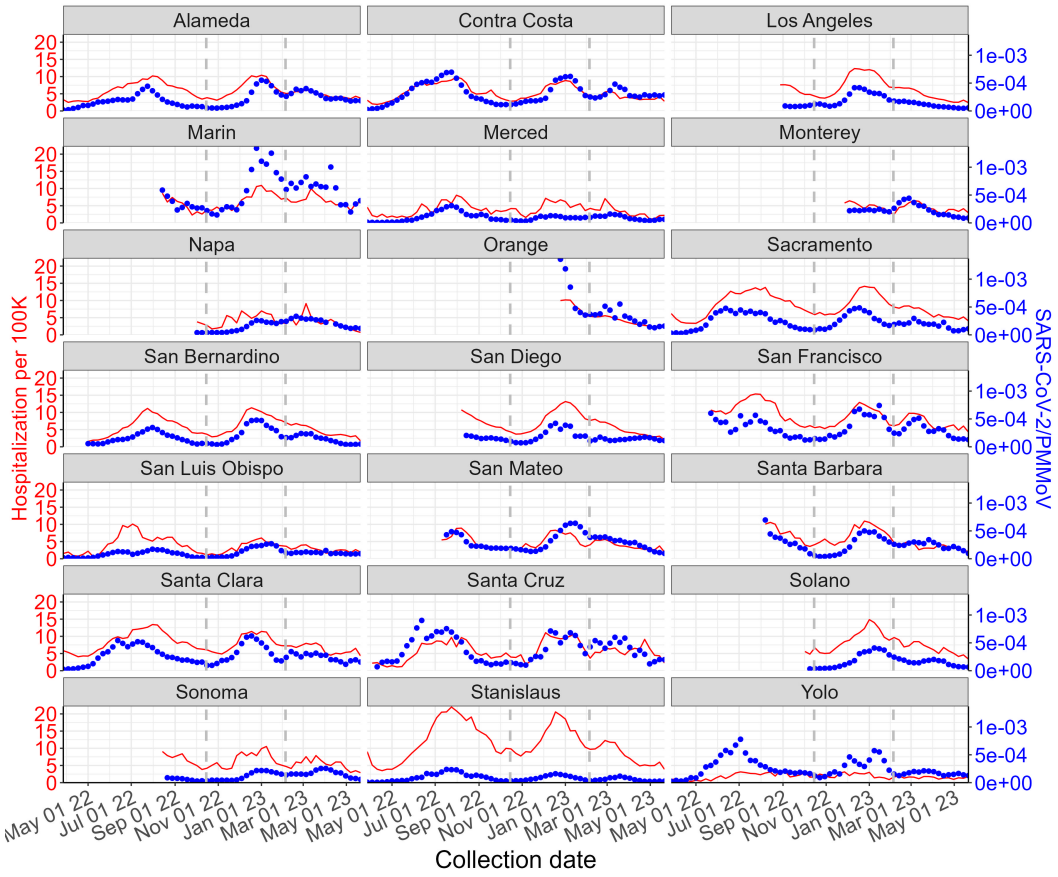

Figure 1: COVID-19 hospitalizations per 100K population (red line) and normalized SARS-CoV-2 WW concentrations (blue dots) from March 21, 2022, to May 21, 2023, by county. Vertical gray lines represent the end of each wave.

2.2 Data Analysis

This study focused on associations between hospitalization rates and longitudinal changes in the SARS-CoV-2 wastewater concentration over time. COVID-19 hospitalization data have been collected repeatedly from counties over time; the traditional linear regression model may not be appropriate due to the presence of correlated measurements within each county. Longitudinal studies often involve correlated data points, and the assumption of independence in linear regression is violated. LMMs allow us to explicitly model the dependence between observations within counties by incorporating random effects. We applied a logarithmic transformation to the weekly average wastewater data and hospitalization rates to facilitate the analysis.

We hypothesized that SARS-CoV-2 wastewater concentration's relation with hospitalization rate varies by county. This hypothesis is based on county-to-county differences in public health recommendations, public health access, and human behavior (Figure 2). We also sought to consider the impact of time-dependent factors associated with each wave of infections. Time-dependent factors include virus variant evolution, human behavior changes, community vaccination status, and prior immunity. We accounted for these factors by incorporating a fixed effect into the model for discrete time periods associated with each wave of infections surveilled in this study (Figure 3).

Kadonsky et al. (2023) observed that the wastewater-to-hospitalization ratios remained relatively stable during two COVID-19 waves in two geographically adjacent counties in California's Central Valley between October 2021 and September 2022. This suggests that the wastewater-to-hospitalization ratios may remain constant in some cases, but the intercept may differ.

Finally, we explore the predictive capabilities of different COVID-19 transmission indicators —including reported cases, TPR, and wastewater data— to determine the most effective real-time indicator to monitor hospitalizations within a region of study.

2.3 Mathematical Model

The log-transformed COVID-19 hospitalization rate at the county $i = 1, \ldots, 21$ and week $t = 1, \ldots, T$ is modelled as

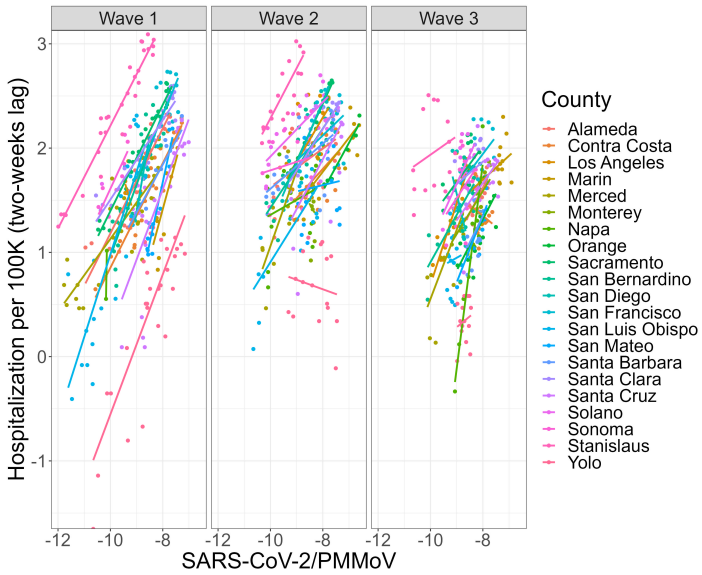

Figure 2: Log transformation of COVID-19 hospitalization rate two-week lagged versus log transformation of the normalized wastewater concentration separated by wave. Regression lines are fitted to the data and depicted; model intercepts and slopes vary by county.

$$y_{it} = \mu + \mathbf{x}_i\boldsymbol{\beta} + v_t + g_i + Z_{it}v_t + \varepsilon_{it} \tag{1}$$

where μ is the average hospitalization rate across the study area and $\mathbf{x}_i$ is a vector of p covariates (e.g., wastewater concentration, reported cases, TPR; $\mathbf{x}_i = \{x_{1it}, x_{2it}, \ldots x_{pit}\}$). The v_t term is a temporal-level fixed effect indicating the pandemic's three waves (grouped time component) as specified above. The g_i term is a county-level random effect corresponding to the county where the hospital is located. County-level random effects are modeled as $g_i \sim N(0, \sigma_g^2)$, with $i = 1, \ldots, 21$. The term $Z_{it}v_t$ represents an interaction effect between a covariate Z_{it} (e.g., wastewater concentration) and the wave factor. The ε_{it} term represent the residuals distributed as $N(0, \sigma^2)$ with σ^2 is the measurement error variance. The random effect g_i is assumed to be independent of the residual ε_{it}.

2.4 Model Implementation

The primary objective of this study is to evaluate our model's ability to predict hospitalizations two weeks in advance using data from wastewater. A two-week lag was incorporated to capture

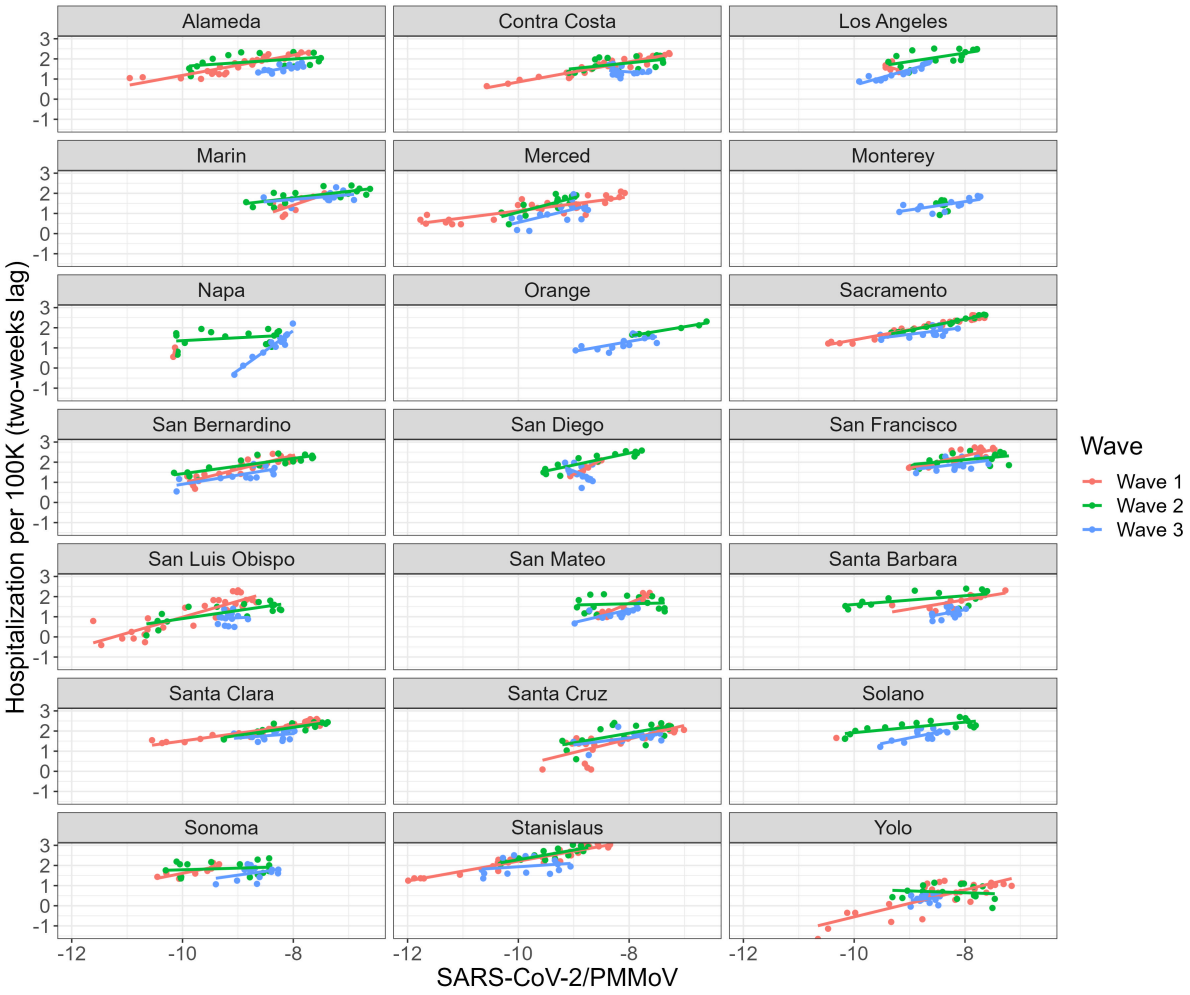

Figure 3: Log transformation of COVID-19 hospitalization rate two-week lagged and log transformation of the normalized wastewater concentration by county. Regression lines are fitted for each county and wave.

the relationship between predictor variables and hospitalization outcomes more accurately. This lag duration was chosen based on previous research showing a nearly two-week delay between hospitalizations and measurements of wastewater, confirmed cases, and test positivity rate (Kadonsky et al., 2023; Montesinos-López et al., 2021). Specifically, we used the hospitalization data two weeks ahead (denoted as Y_i) as the response variable for concentration, cases, and TPR at time i. While a single lag was selected in building the present model, the duration of the lag could be optimized for each county.

In order to account for the interdependence in hospitalization data, all models presented below

will consider the variable "county" (i.e., the county where the hospital is situated) as a random effect in the predictor. The LMMs were executed using the "lme" function from the "nlme" package in R.

2.5 Model Evaluation

We tested 9 statistical prediction models to assess the model's forecasting accuracy. We used the mean absolute scaled error (MASE) as our benchmark. To create these models, we used different predictors in Equation 1, including the number of confirmed cases (cases), TPR, N gene concentration (N), normalized N gene concentration (N/PMMoV), a wave factor (wave), and an interaction effects between normalized concentration and the wave factor (N/PMMoV×wave). The wave factor was added to account for several factors related to the emergence of a new variant, which cannot be measured directly.

The models M1, M2, M3, and M4 assume fixed effects predictor variables for cases, TPR, N gene concentration, and normalized N gene concentration, respectively. All four models also consider a county-level random effect. Models M5, M6, M7, and M8 add a wave effect factor to models M1, M2, M3, and M4, respectively. Model M9 is similar to model M8 but includes an interaction term between N/PMMoV and the wave factor. A summary of these models and their comparative metrics are presented in Table 1.

To evaluate the performance of the models, we used ten-fold cross-validation. The data was split into training and testing sets at random. The training set received 80% of the data, while the testing set was allocated 20%. The model was created using the training set, and its prediction performance was evaluated using the test set. This process was repeated 10 times, creating 10 random partitions. The overall prediction performance was reported as the average of the 10 partitions.

The MASE was used to compare the observed values with the forecasted values to measure the accuracy of predictions. The MASE was computed across 10 partitions, $\text{MASE} = \frac{1}{10}\sum_{k=1}^{10}\text{MASE}_k$, where MASE_k of the k-th fold is estimated by

$$\text{MASE}_k = \frac{\frac{1}{J}\sum_{j}^{J}|y_j - \hat{y_j}|}{\frac{1}{T-1}\sum_{t=2}^{T}|y_t - y_{t-1}|}$$

where y_t and $\hat{y}_t$ represent the observed and predicted values at time t, respectively. The Akaike Information Criteria (AIC) and Bayesian Information Criteria (BIC) were used to evaluate the goodness of fit, with lower values of AIC and BIC indicating superior model fit.

3 Results

Nine models were implemented to predict the number of COVID-19 hospitalizations in 21 counties across California (Table 1). We used the mean absolute scaled error (MASE) as a measure of the accuracy of the model forecasts. We calculated percent differences in MASE between corresponding models to highlight the effect of each covariate tested (Table 1 and Figure A.1). Models using TPR (M2 and M6) demonstrated the best performance overall. These models retroactively used the best measures of TPR, based on collection dates of clinical specimens. In real-time, measures of TPR are delayed by reporting times and may underperform when testing levels are overall low. Models that used wastewater data for hospitalization forecasts (models M3, M4, M7, M8, and M9) were considered successful for hospitalization forecasting when compared to models based on the traditional COVID-19 cases.

Adding a time-dependent factor for each wave of infections (models M5-M8) significantly enhanced forecasting accuracy compared to models without this factor (models M1-M4). Out of all these models, M5 showed the greatest improvement with the incorporation of a wave factor (25% better than M1), while M6 showed the least improvement with the addition of a wave factor (6.4% better than M2). Adding a wave effect to M3 and M4 improved performance by 12.1% and 14.6%, respectively. Normalization with PMMoV (model M8) did not improve prediction performance relative to the model that used unnormalized concentrations (model M7). We found that M2, based on TPR, outperformed models M1, M3, and M4 by 27.7%, 29.3%, and 32.6%, respectively. Models M1, M3, and M4 exhibited comparable prediction performance.

Model M9, which included an interaction effect between normalized concentration and the wave factor, did not improve compared to Model 8.

A cursory assessment of adding interaction terms to models M5 (casesxwave), M6 (TPRxwave), and M7 (Nxwave) indicated that these interaction terms also did not enhance model performance.

Table 1: Model prediction performance based on the mean absolute scaled error (MASE), across 10 random partitions, assuming 80% of the total data set for training and the remaining 20% for testing. The Akaike Information Criteria (AIC) and Bayesian Information Criteria (BIC) are also presented.

Model	**MASE****	**AIC**	**BIC**
M1 = Cases + County*	0.976 (0.075)	872	891
M2 = TPR + County*	0.764 (0.063)	417	437
M3 = N + County*	0.988 (0.071)	845	864
M4 = N/PMMoV + County*	1.013 (0.071)	804	824
M5 = M1 + Wave	0.781 (0.069)	550	579
M6 = M2 + Wave	0.718 (0.067)	327	356
M7 = M3 + Wave	0.881 (0.078)	641	670
M8 = M4 + Wave	0.884 (0.08)	634	664
M9 = M8 + N/PMMoV×Wave	0.863 (0.077)	619	658

∗ Included as a random effect.
∗∗ Mean (standard deviation).

The hospitalization rate predictions for California counties, based on Model M8, are presented in Figure 4. The predicted hospitalization rates align closely with the observed data, indicating that the forecasting model is performing well. Predictions for models M5, M6, and M7 are presented in Figs. B.1, B.2, and B.3, respectively.

4 Discussion

Wastewater-based disease surveillance (WDS) models have been shown to be effective tools to estimate SAR-CoV-2 prevalence and effective reproductive numbers. WDS data has also been shown to correlate with hospitalizations. Our study demonstrates the feasibility of using WDS to reliably forecast hospitalizations at a county level, with a level of accuracy comparable to what we observed when using only confirmed cases or test positivity rates for hospitalization forecasting. The model forecasts yielded promising outcomes for WDS programs in 21 California counties, encompassing 13 million people across the state. Our findings thus offer a promising mechanism to improve real-time monitoring of infectious diseases using wastewater data and to support control

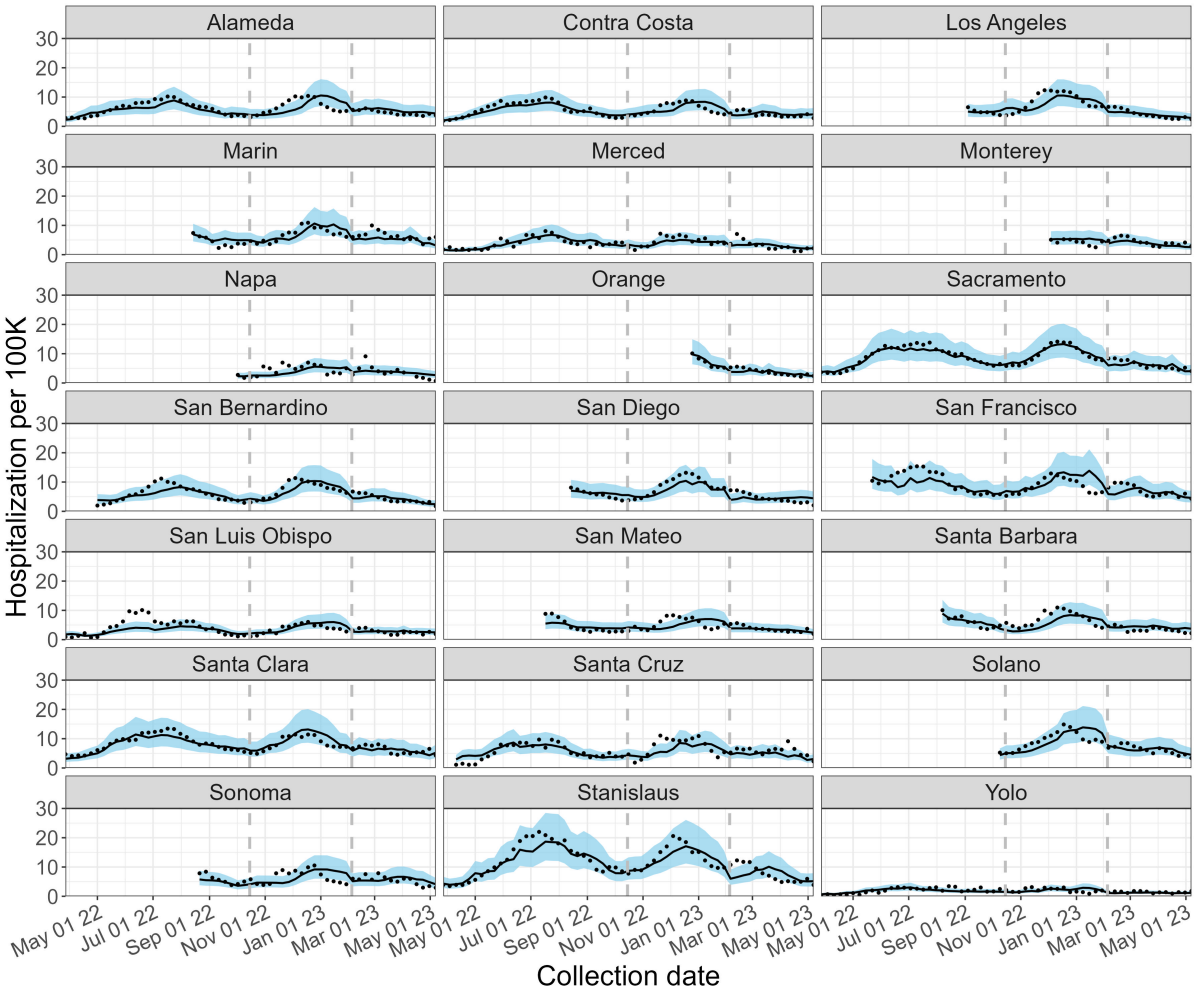

Figure 4: Estimated COVID-19 hospitalization rate based on Model 8. Black-solid lines and blue-shadow area describe the mean and 80% prediction intervals, respectively. Black dots represent the observed data. Vertical gray lines represent the end of each wave.

measures for infectious diseases, especially when clinical testing is limited.

The mixed-effects models we developed facilitate evaluation of the associations between hospital admission rates for COVID-19 and three predictors: confirmed cases, TPR, and the concentrations of SARS-CoV-2 RNA in wastewater. We also introduced a time-dependent factor to account for the wave of infection underway. The wave factor recognizes the non-autonomous nature of the extended COVID-19 pandemic. The duration and spread of the disease through time are influenced by diverse elements including viral variant evolution, human behavior, vaccine development and uptake, prior immunity status, health interventions utilized, and other time-dependent variables.

Inclusion of a wave factor enhanced the accuracy of all models tested. Model M6, which uses both TPR and the wave factor, yielded the strongest prediction performance amongst the nine models tested (lowest mean absolute scaled error). These findings echo previous research showing that TPR serves as a more reliable indicator of disease transmission than confirmed case counts (Dallal et al., 2021). Wastewater data yielded hospitalization forecasts with similar accuracy to models based on traditional testing data, indicating the significant potential for WDS programs to inform hospital capacity planning and resource allocation.

There are several limitations of our study. First, limitations of the hospitalization data must be recognized. Hospitalization data solely reflects the count of individuals who received a COVID-19 diagnosis while at the hospital. The hospitalization dataset thus includes individuals admitted to the hospital for reasons unrelated to COVID-19 but who tested positive during their hospital stay. It was not possible for us to disentangle hospitalizations that were not associated with COVID-19. Second, only 12 counties in the study had wastewater data for all three waves of infection that occurred during the study timeframe. As longer-term WDS datasets become available, future studies should continue to explore the effect of time-dependent factors associated with recurrent waves of infections. Third, our models did not incorporate interrelationships between communities or sewersheds (the areas covered by wastewater collection systems). We initially included a regional factor in the model, using regional classifications (Northern California, Greater Sacramento Region, San Joaquin Valley, San Francisco Bay Area, and Southern California). This broad geographic factor did not result in significant improvements in model performance and was eliminated in favor of model simplicity. More nuanced consideration of spatial correlation structures should be considered in future studies to assess the role of community interconnectivity and geographic proximity on disease dynamics. Finally, we recommend future studies incorporate an adaptive modeling framework. Adaptive frameworks that adjust model parameters according to new developments can generate more reliable and up-to-date forecasting to help decision-makers implement timely interventions.

Since the COVID-19 pandemic is no longer classified as a public health emergency, testing rates have diminished, and measures taken to control the spread of the disease have been curbed. Recent increases in COVID-19 cases and hospitalizations serve as a reminder to maintain vigilance. It is clear that WDS is a valuable tool for real-time disease monitoring, prevention, and preparedness.

Using WDS to forecast hospitalizations offers an efficient method to translate early warning signals from wastewater into public health response strategies. By forecasting hospitalizations two weeks in advance, hospitals can be more proactive in managing their capacity to ensure that all patients receive the care they need. WDS infrastructure is also now being harnessed to monitor a suite of other infectious diseases. We believe there is tremendous potential to extend this approach toward other disease targets to inform hospital planning and public health decision-making.

Availability Statement

All code and underlying data are publicly available through the GitHub repository (https://github.com/Cricelio23/Hospitalization_WW). Analyses were carried out using R version 4.2.2.

Declaration of competing interest

The authors declare that they have no known competing financial interests or personal relationships that could have appeared to influence the work reported in this paper.

Credit author statement

M.L.D.T and **J.C.M.L.**: Conceptualization, Methodology, Software, Formal analysis, Writing - Original draft preparation, Writing - Reviewing & Editing. **A.N.D**, **C.C.N.**, and **H.N.B.**: Conceptualization, Writing - Reviewing & Editing. **M.N.**: Conceptualization, Methodology, Supervision, Writing - Reviewing & Editing.

References

A. B. Boehm, B. Hughes, D. Duong, V. Chan-Herur, A. Buchman, M. K. Wolfe, and B. J. White. Wastewater concentrations of human influenza, metapneumovirus, parainfluenza, respiratory syncytial virus, rhinovirus, and seasonal coronavirus nucleic-acids during the covid-19

pandemic: a surveillance study. *The Lancet Microbe*, 4(5):e340–e348, 2023a. doi: 10.1016/S2666-5247(22)00386-X.

A. B. Boehm, M. K. Wolfe, K. R. Wigginton, A. Bidwell, B. J. White, B. Hughes, D. Duong, V. Chan-Herur, H. N. Bischel, and C. C. Naughton. Human viral nucleic acids concentrations in wastewater solids from central and coastal california usa. *Scientific Data*, 10(1):396, 2023b. doi: 10.1038/s41597-023-02297-7.

A. A. Dallal, U. AlDallal, and J. A. Dallal. Positivity rate: an indicator for the spread of covid-19. *Current Medical Research and Opinion*, 37(12):2067–2076, 2021. doi: 10.1080/03007995.2021.1980868. URL https://doi.org/10.1080/03007995.2021.1980868. PMID: 34517740.

M. L. Daza-Torres, J. C. Montesinos-López, M. Kim, R. Olson, C. W. Bess, L. Rueda, M. Susa, L. Tucker, Y. E. García, A. J. Schmidt, C. C. Naughton, B. H. Pollock, K. Shapiro, M. Nuño, and H. N. Bischel. Model training periods impact estimation of covid-19 incidence from wastewater viral loads. *Science of The Total Environment*, 858:159680, 2023. ISSN 0048-9697. doi: 10.1016/j.scitotenv.2022.159680.

D. Dowdy and G. D'Souza. Covid-19 testing: understanding the "percent positive". *Johns Hopkins Bloomberg School of Public Health*, 2020. URL https://publichealth.jhu.edu/2020/covid-19-testing-understanding-the-percent-positive.

L. Fenga and M. Gaspari. Predictive capacity of covid-19 test positivity rate. *Sensors*, 21(7), 2021. ISSN 1424-8220. doi: 10.3390/s21072435. URL https://www.mdpi.com/1424-8220/21/7/2435.

A. Galani, R. Aalizadeh, M. Kostakis, A. Markou, N. Alygizakis, T. Lytras, P. G. Adamopoulos, J. Peccia, D. C. Thompson, A. Kontou, A. Karagiannidis, E. S. Lianidou, M. Avgeris, D. Paraskevis, S. Tsiodras, A. Scorilas, V. Vasiliou, M.-A. Dimopoulos, and N. S. Thomaidis. Sars-cov-2 wastewater surveillance data can predict hospitalizations and icu admissions. *Science of The Total Environment*, 804:150151, 2022. ISSN 0048-9697. doi: https://doi.org/10.1016/j.scitotenv.2021.150151. URL https://www.sciencedirect.com/science/article/pii/S0048969721052281.

B. Hughes, D. Duong, B. J. White, K. R. Wigginton, E. M. G. Chan, M. K. Wolfe, and A. B. Boehm. Respiratory syncytial virus (rsv) rna in wastewater settled solids reflects rsv clinical positivity rates. *Environmental Science & Technology Letters*, 9(2):173–178, 2022. doi: 10.1021/acs.estlett.1c00963. URL https://doi.org/10.1021/acs.estlett.1c00963.

K. F. Kadonsky, C. Naughton, R. Olson, M. Susa, S. G.L., M. Nuno, J. Daza-Torres, M.L. andf Montesinos-López, et al. Expansion of wastewater-based disease surveillance to improve health equity in california's central valley: sequential shifts in case-to-wastewater and hospitalization-to-wastewater ratios. *Frontiers in Public Health*, 11, 2023. doi: 10.3389/fpubh.2023.1141097.

T. Kumblathan, Y. Liu, G. K. Uppal, S. E. Hrudey, and X.-F. Li. Wastewater-based epidemiology for community monitoring of sars-cov-2: Progress and challenges. *ACS Environmental Au*, 1(1):18–31, 2021. doi: 10.1021/acsenvironau.1c00015. URL https://doi.org/10.1021/acsenvironau.1c00015.

J. C. Montesinos-López, M. L. Daza-Torres, Y. E. García, L. A. Barboza, F. Sanchez, A. J. Schmidt, B. H. Pollock, and M. Nuño. The role of sars-cov-2 testing on hospitalizations in california. *Life*, 11:1336, 2021. doi: 10.3390/life11121336.

J. C. Montesinos-López, M. L. Daza-Torres, Y. E. García, C. Herrera, C. W. Bess, H. N. Bischel, and M. Nuño. Bayesian sequential approach to monitor covid-19 variants through test positivity rate from wastewater. *mSystems*, 0(0):e00018–23, 2023. doi: 10.1128/msystems.00018-23. URL https://journals.asm.org/doi/abs/10.1128/msystems.00018-23.

J. R. Paul, J. D. Trask, and S. Gard. Ii. poliomyelitic virus in urban sewage. *The Journal of Experimental Medicine*, 71(6):765–77, 1940. doi: 10.1084/jem.71.6.765.

K. K. To, K.-H. Chan, I. W. Li, T.-Y. Tsang, H. Tse, J. F. Chan, I. F. Hung, S.-T. Lai, C.-W. Leung, Y.-W. Kwan, Y.-L. Lau, T.-K. Ng, V. C. Cheng, J. S. Peiris, and K.-Y. Yuen. Viral load in patients infected with pandemic h1n1 2009 influenza a virus. *Journal of Medical Virology*, 82(1):1–7, 2010. doi: https://doi.org/10.1002/jmv.21664. URL https://onlinelibrary.wiley.com/doi/abs/10.1002/jmv.21664.

J. D. Trask, A. Vignec, and J. R. Paul. Poliomyelitis virus in human stools. *Journal of the American Medical Association*, 111(1):6–11, 1938. doi: 10.1001/jama.1938.02790270008002.

Verily. Wastewater testing dashboard. URL http://publichealth.verily.com/?v=SC2_N&l=Coeur+d%27Alene%2C+IDh. (Accessed on 05/23/2023).

WastewaterSCAN. Wastewaterscan dashboard. URL https://data.wastewaterscan.org/tracker. (Accessed on 05/23/2023).

Appendices

A Prediction performance

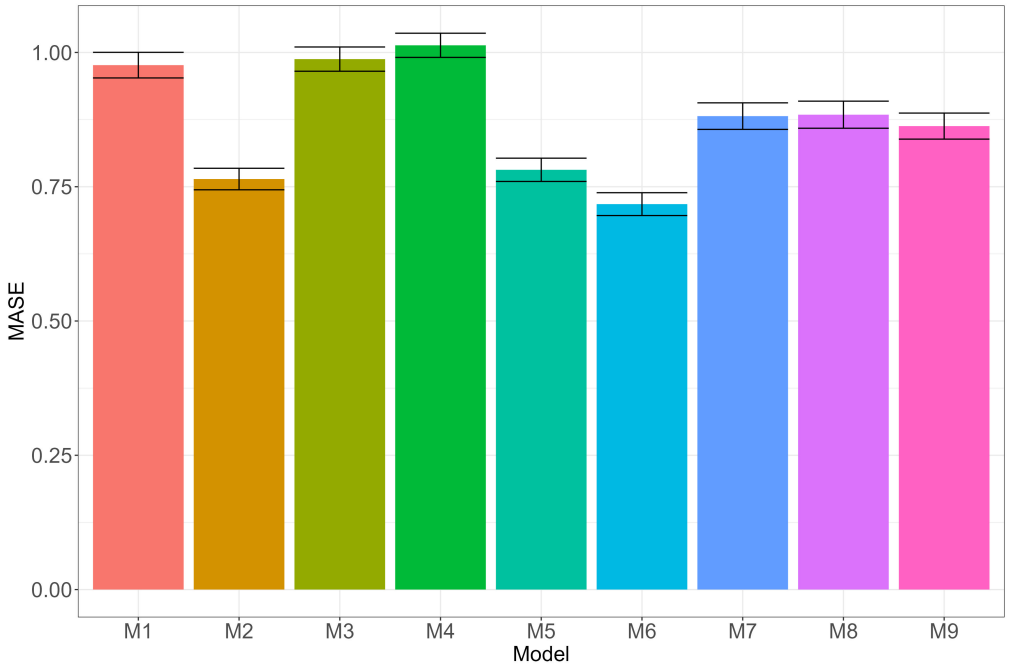

Figure A.1: **Performance prediction of models described in Table 1:** mean absolute scaled error (MASE) with its standard deviation across the 10 partitions.

B Predictions of models M5, M6, and M7

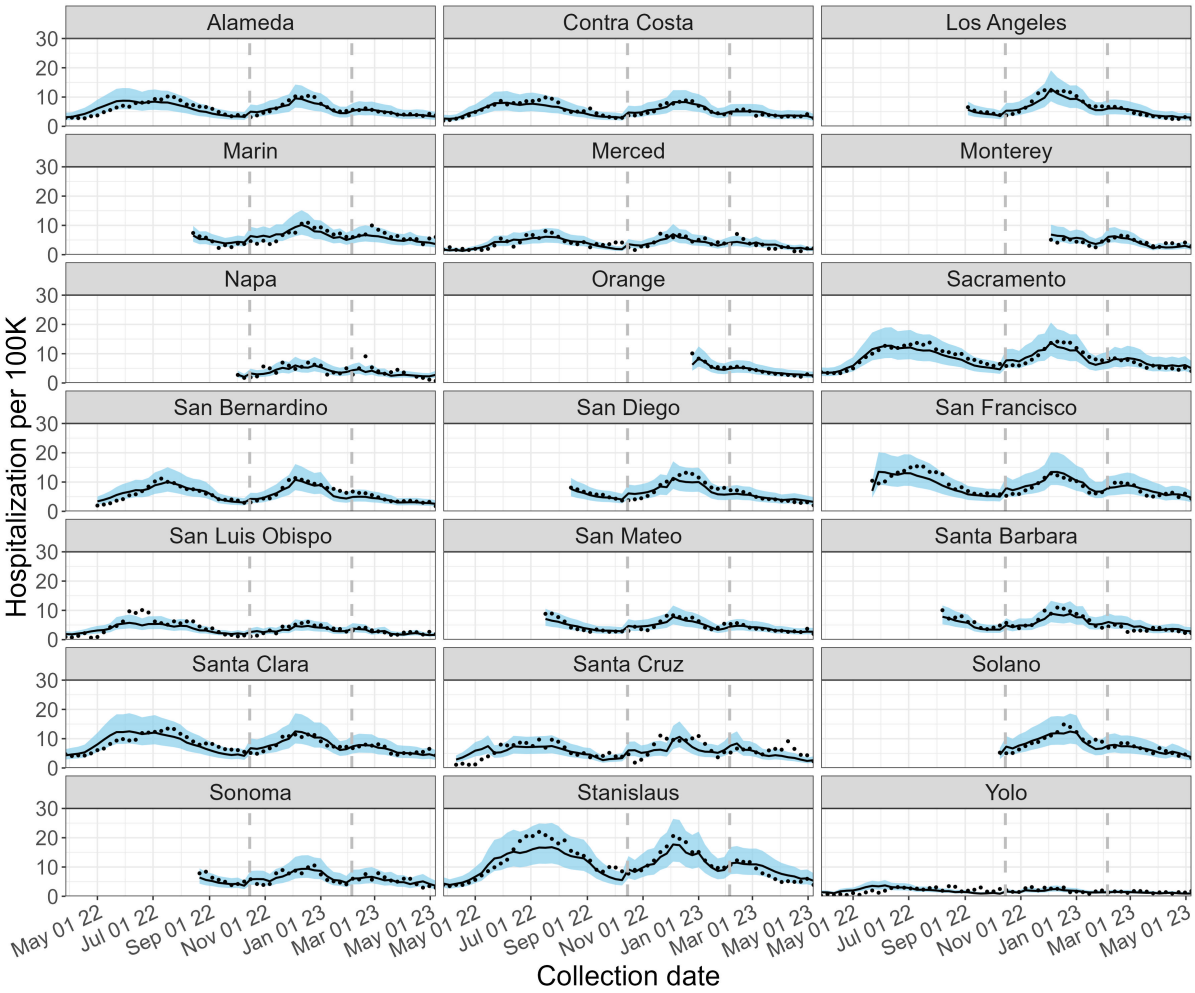

Figure B.1: **Model M5 = Cases + wave + County.** Estimated COVID-19 hospitalization rate. Black-solid lines and blue-shadow area describe the mean and 80% prediction intervals, respectively. Black dots represent the observed data. Vertical gray lines represent the end of each wave.

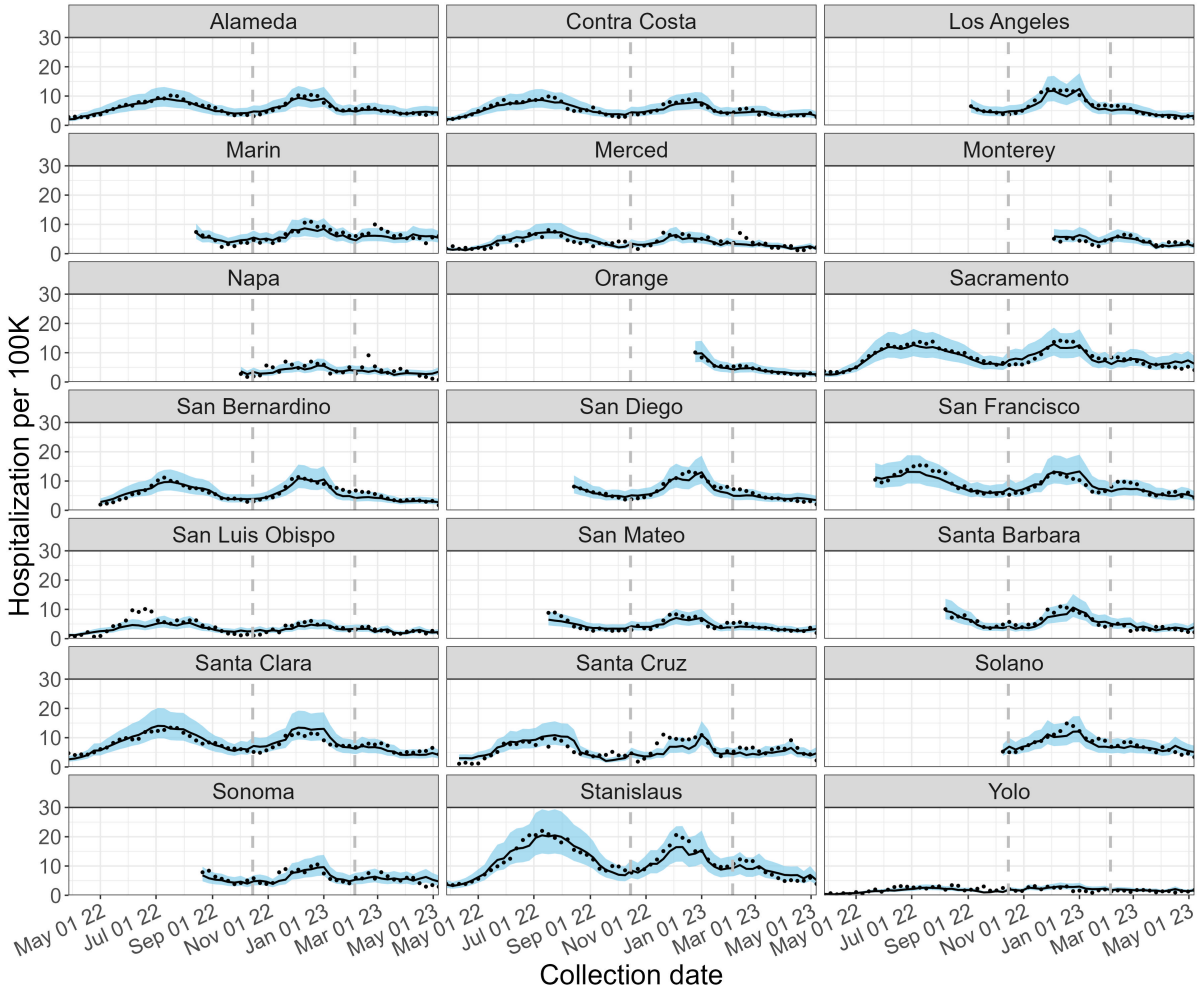

Figure B.2: **Model M6 = TPR + wave + County.** Estimated COVID-19 hospitalization rate. Black-solid lines and blue-shadow area describe the mean and 80% prediction intervals, respectively. Black dots represent the observed data. Vertical gray lines represent the end of each wave.

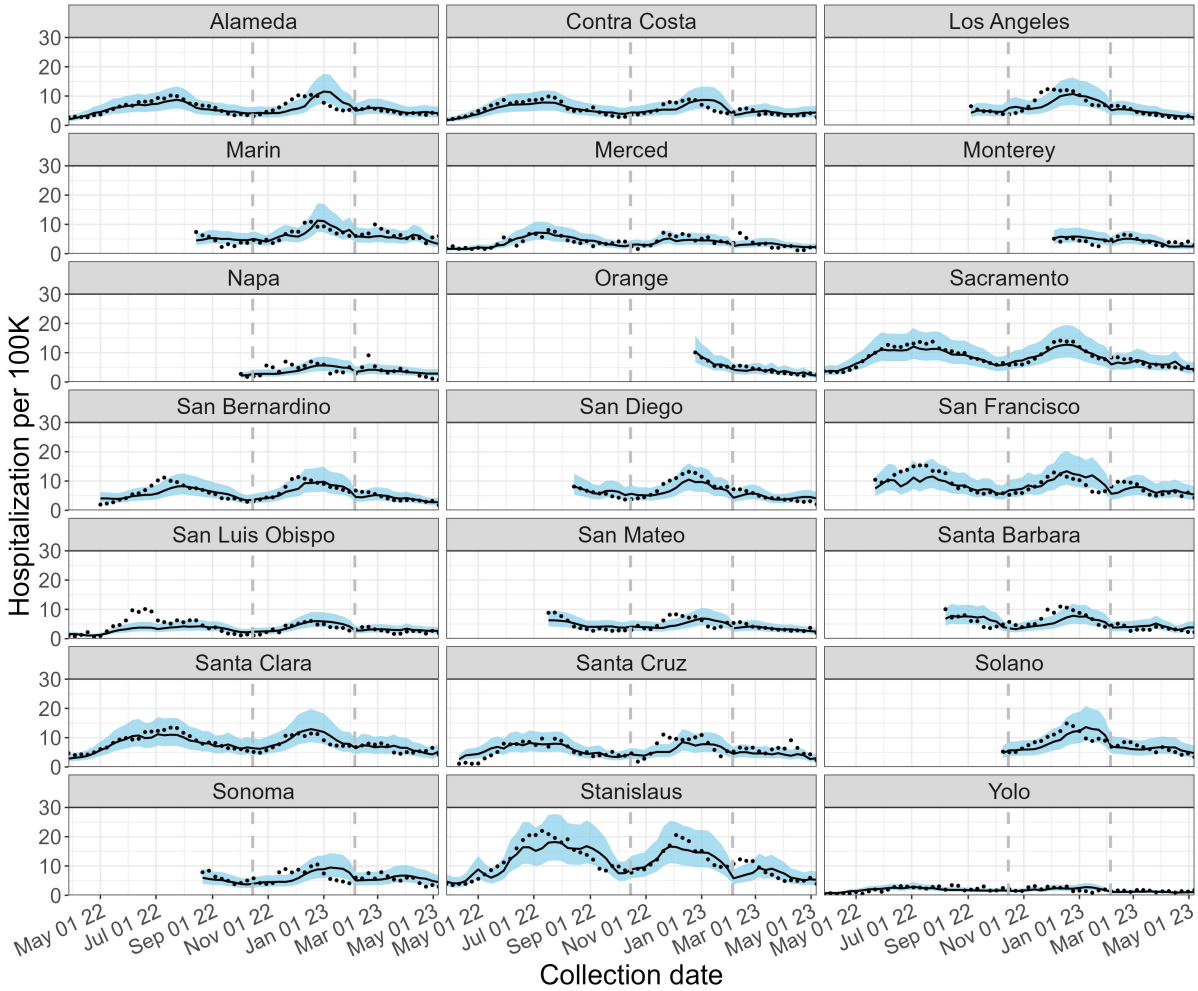

Figure B.3: **Model M7 = N + wave + County.** Estimated COVID-19 hospitalization rate. Black-solid lines and blue-shadow area describe the mean and 80% prediction intervals, respectively. Black dots represent the observed data. Vertical gray lines represent the end of each wave.